Food Chemistry: X 19 (2023) 100759

Contents lists available at ScienceDirect

Food Chemistry: X

journal homepage: www.sciencedirect.com/journal/food-chemistry-x

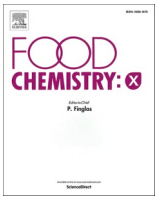

The freeze-thaw stability of flavor high internal phase emulsion and its application to flavor preservation and 3D printing

Sijie Hu, Feng Xiao, Ming Du, Jinfeng Pan, Liang Song, Chao Wu, Beiwei Zhu *, Xianbing Xu *

National Engineering Research Center of Seafood, Collaborative Innovation Center of Provincial and Ministerial Co-construction for Seafood Deep Processing, School of Food Science and Technology, Dalian Polytechnic University, Dalian 116034, PR China

ARTICLE INFO

Keywords:
High internal phase emulsion
Freeze–thaw stability
Flavor substance preservation
3D printing

ABSTRACT

Volatilization of flavor substances may reduce consumers' perception of flavor, and the research on preservation of flavor substances by high internal phase emulsions (HIPEs) under freeze–thaw conditions is still blank. Herein, flavor HIPEs prepared by adding more than 15% litsea cubeba oil in the oil phase could be used as food-grade 3D printing inks, and showed better stability after 5 freeze–thaw cycles, which could be interpreted as the reduced ice crystal formation, more stable interface layer, and more flexible gel-like network structure resulting from the protein binding to flavor substances. The constructed HIPEs system in this study could preserve the encapsulated flavor substances perfectly after 5 freeze–thaw cycles. Overall, this study contributes a food-grade 3D printing ink, and provides a new method for the preservation of flavor substances under freezing conditions and expands the application range of flavor HIPEs in food industry.

1. Introduction

Flavor is one of the most important characteristics of food, and desirable flavor properties is beneficial to enhance the purchasing power of consumers. However, the volatilization of flavor substances may reduce consumers' perception of flavor. It is a big challenge for researchers to design flavor preservation and delivery system, as flavor release is influenced by both food ingredients and food structures (Mao et al., 2017).

At present, the encapsulation of flavor compounds by emulsion system is one of the most effective methods, which can preserve or masking flavor compounds, and improve their thermal stability, oxidation stability and bioavailability (Saifullah et al., 2019). In addition, emulsion system can also overcome the restriction of high volatility of flavor substances, and increase their application in food system (Saifullah et al., 2019). Emulsion stabilized by particles has been widely reported to be used for the encapsulation and preservation of flavor substances. Wu et al. (K. Wu et al., 2022) used soy protein isolate modified by tannic acid as a stabilizer for emulsion encapsulated flavor compounds. Polymeric nanoparticles and biopolymers particles have also been reported in encapsulate the flavor compounds (Manfredini et al., 2021; Marcuzzo et al., 2012). Nevertheless, compared with conventional liquid emulsions, high internal phase emulsions (HIPEs) exhibited higher load rate, thus has greater potential for preservation and delivery for flavor compounds.

HIPEs is a kind of highly concentrated gel-like emulsion which was named for its extremely high internal phase ratio (≥74%) by Lissant (Lissant, 1966) in 1966. HIPEs has long been a very attractive materials with a range of applications in food, such as sauces, cream products, fat substitutes and nutrient delivery system (Liu et al., 2018). However, there are few research on encapsulation of flavor substances with high internal phase emulsions (HIPEs). Wu et al. (X. Wu et al., 2022) found that HIPEs based on glycyrrhizic acid and phytosterol could tuned the flavor release, and could be applied to fat substitutes in meat alternatives. Furthermore, whether eaten directly (e.g., ice cream) or as a fat substitute in minced meat products, the freezing process is hardly to be avoided for HIPEs preservation.

As a two-phase system, freeze–thaw destabilization has always been a major problem for the application of HIPEs. The freeze–thaw instability of HIPEs might cause the layer surrounding individual oil droplets rupturing, and allow the oil droplets to coalesce rapidly, thereby resulting in the separation of HIPE into original aqueous and oil phase (Ghosh & Coupland, 2008), which greatly destroys the encapsulation of flavor substances. At present, conjugate consisting of protein and sugar seems to be one of the most effective stabilizers for improving the freeze–thaw stability of emulsions. it was previously found by the

* Corresponding authors.
E-mail addresses: zhubeiwei@163.com (B. Zhu), xianbingxu@gmail.com (X. Xu).

https://doi.org/10.1016/j.fochx.2023.100759
Received 19 April 2023; Received in revised form 9 June 2023; Accepted 16 June 2023
Available online 17 June 2023

present study group that galactooligosaccharide/glycosylated cod protein produced the freeze–thaw stable HIPEs with low glycemic index (unpublished resorts). However, the freeze–thaw stability of flavor HIPEs and the retention of flavor substances during freeze–thaw process have not been reported.

Three-dimensional printing (3D printing) is an additive manufacturing process that creates physical structure by continuously rolling out multi-layer materials aided by 3D digital models (Ali et al., 2022). In recent years, the application of 3D printing has been increasing, due to its advantages of personalized customization, product beautification and low level of operation technology (Petrovic et al., 2010). However, the initial applications of this technology are mainly to produce custom innovative materials with novel properties, such as plastics or metal products (Enfield et al., 2022), hence traditional 3D printing inks lack the biocompatibility and biodegradability to be used in food industry or drug delivery systems (Li et al., 2020). As a material with extrusion shear thinning ability, high shear elastic modulus and high shear yield strength, HIPEs is considered as a potential 3D printing ink (Sears et al., 2016). Bi et al. (A. Bi et al., 2022) provided an excellent 3D printing ink, O/W HIPEs with strong gel strength stabilized by casein/pectin particles, and the printed objects fully retained the preset structure and shape. Additionally, food-grade HIPEs stabilized by gelatin/cyanobacteria protein (Wang et al., 2022), rice protein/carboxymethyl cellulose (Wan et al., 2021), and gelatin crosslinked by glutamine transaminase (Du et al., 2021) have also been reported as 3D printing inks. The application of freeze–thaw stable flavor HIPEs to 3D printing helps to enhance the customization and aesthetics of frozen products. To date, there are no reports of freeze–thaw stability of 3D printing products using flavor HIPEs.

Herein, litsea cubeba oil with strong and volatile flavor was used in production of freeze–thaw stable flavor HIPEs. The effects of flavor substances on the freeze–thaw stability of HIPEs were discussed, and the preservation of volatile flavor substances during freeze–thaw process was demonstrated. Furthermore, the food-grade flavor 3D printing object with freeze–thaw stability was produced. To the best of our knowledge, this is the first report of HIPEs preserving volatile flavor substances during freeze–thaw process, which was an important step to preserve flavor substances in the frozen environment. In addition, this is also the first report on the freeze–thaw stability of 3D printing object prepared by food-grade flavor HIPE.

2. Materials and methods

2.1. Materials

The cod protein (CP, 912.2 g/kg of protein) was extracted from *Theragra Chalcogramma* according to the method reported by Li et al. (Li et al., 2020). Bicinchoninic acid Protein Assay Kit (BCA kit) was purchased from Solarbio Science & Technology Co., Ltd. (Beijing, China). HCl and NaOH (both analytical grad) were purchased from Damao Chemical Reagent Co., Ltd. (Tianjin, China). Soybean oil was purchased from a local supermarket (Dalian, China). Litsea cubeba oil extracted from the fruits of *Litsea cubeba* was purchased from Dasheng Seasoning Food Factory (Lengshuijiang, China).

2.2. Preparation of the complex of galactooligosaccharide and glycosylated cod protein (GOS-GCP)

Lyophilized CP was redissolved by distilled water with the CP concentration of 5%. The pH of the CP solution was adjusted to 10 by 6 M NaOH followed by stirring at room temperature for 5 h. And then, 12% glucose was added to the CP solution. After another hour of stirring, the dispersion was incubated in oil bath at 120 °C for 20 min to obtain Glycosylated cod protein (GCP). The free glucose in GCP was removed by dialysis for 48 h, and the protein concentration of GCP was then tested with BCA kit. Galactooligosaccharide (GOS) was dissolved in the post-dialysis GCP solution with protein/GOS mass ratios of 5:6. After 1 h of hydration, the mixture was lyophilized to obtain the complex of galactooligosaccharide and glycosylated cod protein (GOS-GCP).

2.3. Preparation of flavor HIPEs

A solution of GOS-GCP with protein content of 50 mg/mL was prepared and the pH was adjusted to 8. The flavor oil was mixed by soybean oil and Litsea cubeba oil (the proportion of litsea cubeba oil was 10%, 15%, 20%, 25% and 30%, respectively). Protein solution (4 mg, pH 8) was mixed with 16 mg of flavor oil ($\varphi = 80\%$), and the mixture was sheared at 8,000 g for 90 s using a homogenizer (T25, IKA, Germany). Thereafter, 90 μL of 3 M HCl were added to the mixture, and the mixture was sheared again by homogenizer at 3,000 g for 30 s to obtain flavor HIPEs.

2.4. Freeze-thaw stabilization of flavor HIPEs

The prepared flavor HIPEs (10 mg) were transferred to freezing tubes and isothermally stored in a freezer for 22 h, at −30 °C, following by thawing in a 37 °C water bath for 2 h, which was defined as a freeze–thaw cycle. A total of 5 freeze–thaw cycles were performed, and the status of the HIPEs after each freeze–thaw cycle was recorded by camera.

2.5. The oiling off of flavor HIPEs

Oiling off of flavor HIPEs was measured according to the method of Wang et al. (Wang et al., 2020). 500 g of flavor oil was mixed with 0.0075 g of Sudan III, and then the mixed oil and flavor HIPEs was added to the centrifuge tube in a ratio of 4:1. After centrifuged for 20 min at 16,000 g, the oil was taken out, and the absorbance of oil was measured at 508 nm. The oiling off of flavor HIPEs was calculated according to formula (1):

$$\varnothing = \frac{m_0 \times (a-1)}{m_e \varnothing_d} \times 100\% \quad (1)$$

where m_0 - the mass of mixed oil; m_e - the mass of flavor HIPEs; a - the ratio of the absorbance of mixed oil to the absorbance of oil after centrifugation; φ_d - the mass fraction of oil phase in flavor HIPEs.

2.6. Microstructure of the flavor HIPEs

The HIPE samples were diluted twice with distilled water. The droplet size and the stable state of HIPEs were obtained by observing the micrographs of HIPEs using an E-100 light microscope (Nikon, Japan).

2.7. 3D printing of flavor HIPEs

3D printing of the flavor HIPEs was performed according to the method reported by Dong et al. (Dong et al., 2019). The twenty-layer cylindrical structure was designed by a designed Java program on computer, and the flavor objects were printed using a 3D printer (FPE2, Fochif Mechatronics Technology Co., Ltd, China) at room temperature. Briefly, flavor HIPEs was loaded into the extrusion cylinder and the emulsion was extruded from the nozzle with a diameter of 1 mm at a speed of 1 mm^3/s.

2.8. Freeze-thaw stabilization of 3D-printed flavor HIPEs

The 3D-printed flavor HIPEs were placed in a petri dish and isothermally stored in a freezer for 22 h, at −30 °C, following by thawing in a 37 °C water bath for 2 h. The above freeze–thaw cycle was repeated five times. The status of the 3D printing objects before and after freeze–thaw treatment was recorded by camera.

2.9. Three-phase contact angle

The three-phase contact angle was determined by a drop shape analyzer (DSA 25, KRÜSS, Germany) according to the method reported by Li et al. (Li et al., 2020). 0.1 g of GOS-GCP were pressed into disks in a mortar for 5 min under the pressure of 20 ton/m^2, and the disks were soaked in the flavor oil containing different proportions of litsea cubeba oil for 2 h to fully infiltrate. After dried with kitchen paper, the protein disks were placed on a glass slide. 10 μL of Milli-Q water was squeezed out and suspended from the tip of the syringe. The contact angle of samples was obtained by Advance software (KRÜSS, Germany) according to the shape recorded by the camera at the moment when the disk attached to the water droplet. Each measurement was performed in triplicate.

2.10. Interfacial tension measurement

The interfacial adsorption of protein at the flavor oil–water interface was detected by a drop shape analyzer (DSA 25, KRÜSS, Germany). The flavor oil was placed in a quartz cylinder. A syringe with a diameter of 0.95 mm was inserted into the flavor oil, and 8 μL of the GOS-GCP (the protein content was 50 mg/mL) was squeezed out to suspend in the flavor oil, followed by injecting 1 M HCl (0.5 μL) into the protein droplets. The interfacial tension was recorded at 10-second intervals for a total of 150 times.

2.11. Rheological behavior of the HIPEs

A rheometer (Discovery HR-1, TA, USA) was used to measure the rheological behavior of the HIPEs, and the parallel plate geometry with diameter of 60 mm was used. The linear viscoelastic range of the flavor HIPEs was performed using storage moduli (G′) and loss modulus (G″) in the strain rage of 0.10 and 500 Pa with a constant frequency of 10.00 Hz. The dynamic frequency sweeps were then determined from 0.1 to 10.00 Hz. Regarding apparent viscosity measurements, the shear rate was increased from 0.10 to 100 s^{-1}. All measurements were performed thrice at room temperature.

2.12. Differential scanning calorimetry (DSC)

The thermal behaviors of the flavor HIPEs were evaluated according to the reports of Noshad et al. (Noshad et al., 2015) with some modifications. 10 mg of emulsion was sealed in aluminium crucible and was then loaded into DSC (TA DSC250, USA). An empty crucible was used as a reference. The temperature was cycled from 20 to − 30 °C at 5 °C/min and vice versa. In addition, to further study the thermal behaviors of the HIPEs, the temperature cycle was repeated three times.

2.13. Analysis of volatile compounds of flavor HIPEs

The volatile compounds produced by flavor HIPEs before and after freeze–thaw process were analyzed using Gas Chromatograph-Mass Spectrometer (GC–MS). Flavor HIPEs (0.38 g) was loaded into a 20 mL headspace vial wand was incubated in water bath at 60 °C for 20 min. The SPME fiber (Sigma-Aldrich, St. Louis, Missouri, USA) was then inserted to the headspace vial at 60 °C for 30 min to extracted the volatile compounds. The fiber was then transfer to the injection port of the GC system, and the volatile compounds were thermally desorbed at 240 °C for 17 min. The 7890 A GC system (Agilent Technologies Inc., Santa Clara, California, USA) was equipped with a 15 m × 250 μm column (19091S-431UI, Agilent, USA). The injection port temperature was 240 °C. The GC oven temperature program was set as follows: increase the temperature from the initial 35 °C to 75 °C at a rate of 3 °C/min; maintain the temperature at 75 °C for 3 min; increase temperature to 240 °C at a rate of 5 °C/min; maintain the temperature at 240 °C for 3 min. With the *N*-alkane mixture as the standard sample ($C_7 \sim C_{30}$), the retention index (RI) was calculated according to Formula (2):

$$RI_a = RI_{n-1} + 100 \times (RT_a - RT_{n-1}) \div (RT_{n+1} - RT_{n-1}) \quad (2)$$

where: RI - the retention index; RT - the retention time; T – the time; a - the sample to be tested; n-1 - the *N*-alkane at the occurrence time of the sample to be tested; n + 1 - the next *N*-alkane at the occurrence time of the sample to be tested.

With 2, 3-diethylpyrazine as the internal standard, the relative quantification of flavor release in samples was calculated according to formula (3):

$$m_i = A_i \times m_s \div A_s \div w \quad (3)$$

where: i - the sample to be measured; s - the internal standard; m - the concentration; A - the ion peak area; w - the sample weight.

2.14. Statistical analysis

Mean ± standard deviation was expressed as the results for each treatment. Analysis of variance (ANOVA) was performed to determine any significant differences ($p < 0.05$) using SPSS Statistics 20.

3. Results and discussion

3.1. The freeze–thaw stability of HIPEs

The freeze-thawing stability of HIPEs prepared with different proportions of litsea cubeba oil was evaluated by repeatedly freezing them at −30 °C for 22 h and then thawing them at 37 °C for 2 h. The freeze–thaw stability of HIPEs after 5 freeze–thaw cycles are shown in Fig. 1a. Flavor HIPEs prepared with more than 15% litsea cubeba oil maintained a good emulsion appearance after 5 freeze–thaw cycles, while there was slight emulsion droplet coalescing and oil–water separation phenomenon could be observed in HIPEs with 10% HIPEs litsea cubeba oil. The freeze–thaw stability of HIPEs is largely associated with the stabilization of interfacial layer. One important role of type of lipid is to affect the force generated by the expansion of the ice crystals transferred to the membrane (Palazolo et al., 2011). Therefore, this might be one of the reasons for the different freeze–thaw stability of HIPEs with different proportion of litsea cubeba oil.

The freeze–thaw stability of flavor HIPEs was further analyzed by optical microscope. Due to the hard texture of the prepared HIPEs, all the emulsions were diluted twice in order to prevent the droplets from being crushed. It can be observed from Fig. 1b that the droplets of all HIPEs samples were spherical, with the size of about 2–4 μm, and the distribution of droplets was loose and uniform, while the emulsion with oil phase of soybean oil showed tight accumulation and poor distribution of droplets size. After 1 freeze–thaw cycle, the size of the droplet was almost unchanged, indicating the stability of HIPEs. With the increase of freeze–thaw cycles, the droplets size uniformity of all samples decreased gradually. After 5 freeze–thaw cycles, large droplets increased significantly, which was caused by the agglomeration of droplets resulted from the destruction of the emulsion droplet interface layer during freeze–thaw process (Ghosh & Coupland, 2008). Besides, HIPEs with high concentration of litsea cubeba oil (≥15%) maintained tight-packed network structure after 5 freeze–thaw cycles, reflecting that flavor HIPEs has excellent freeze–thaw stability.

After freeze–thaw treatment of HIPEs, the oil–water interface was damaged by ice crystals, leading to the separation of oil and water phase (Oliver et al., 2009). However, the separation of light degree is hardly to be observed. Therefore, the oiling off of HIPEs after centrifugation was detected, in order to further analyzed the influence of the concentration of litsea cubeba oil on the freeze–thaw stability of HIPEs. According to Fig. 1c, the oiling off of all samples increased obviously with the increase of freeze–thaw cycles. There was no significant difference in the oiling off between the HIPEs with less than three freeze-thawing cycles, while

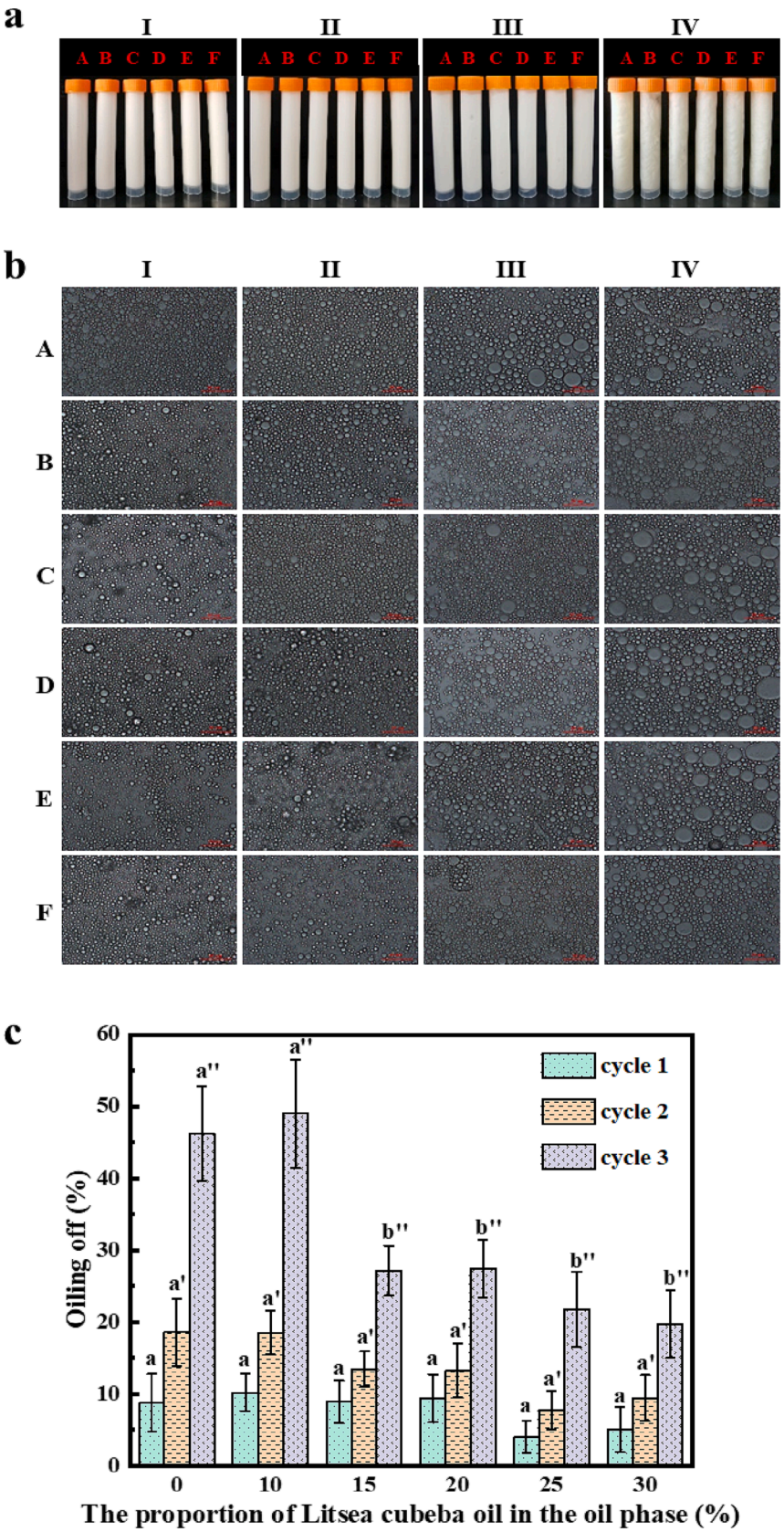

Fig. 1. a: Visual images of HIPEs; b: Microstructures images of HIPEs; c: Oiling off of HIPEs (*A ~ F: HIPEs with 0%, 10%, 15%, 20%, 25% and 30% litsea cubeba oil in the oil phase oil, respectively; I ~ IV: HIPEs after 0, 1, 3 and 5 freeze–thaw cycles; **Different letters of the same superscript indicated significant differences between different samples, $p < 0.05$).

after 5 freeze–thaw cycles, the oiling off of HIPEs with less than 15% litsea cubeba oil increased significantly, indicating that HIPEs prepared with higher litsea cubeba oil content had higher freeze-thawing stability. It was confirmed that the type of oil phase affected the freeze–thaw stability of HIPEs (Palazolo et al., 2011).

3.2. Interpretation for the freeze–thaw stability of flavor HIPE

The freeze–thaw stability of flavor HIPE is mainly attributed to the properties of protein at the oil/water interface, the interaction of emulsion droplets and the formation of ice crystals. The three-phase contact angle and interfacial tension were used to characterizing the properties of proteins at the oil–water interface; rheological behavior of HIPEs was used to analyze the influence of the interaction of emulsion droplets; and DSC was used to explore the formation of ice crystals.

The surface wettability of protein particles is one of the important factors for the construction of stable HIPEs (Atkins et al., 2020). Three-phase contact angle were herein used to describe the wettability of protein particles at the flavor oil/water interface. As shown in Fig. 2a, the surface wettability of proteins soaked in flavor oil was higher than those soaked in soybean oil, which might be related to the higher hydrophobicity of aromatic compounds (Purwanti et al., 2016). In addition, with the increase of litsea cubeba oil concentration, the three-phase contact angle of protein particles increased slightly (from 75° to 81°), indicating that the protein hydrophobicity improved, which might be attribute to the formation of intramolecular hydrogen bonds between the protein hydrophilic groups and flavor compounds. Zhang et al. (Zhang et al., 2022) reported similar results that flavor compounds could change the secondary structure of proteins and form more hydrogen bonds between molecules through the interaction of 2-octenone, 1-octene-3-alcohol and octenal with soy protein isolate, indicating that the proteins had higher amphiphilicity at the flavor oil/water interface and had the ability to construct a more stable HIPEs system.

The interfacial tension of protein particles at the oil–water interface is another key factor of stabilizing HIPEs. Fig. 2b shows the variation of protein tension at the flavor oil/water interface with different litsea cubeba oil concentrations. The diffusion rate of protein to flavor oil/water interface was not different from that of soybean oil/water interface, both showed a rapid decline within 50 s, then a gradual decline trend, and remained stable until 300 s later. However, the interfacial tension of protein at the flavor oil/water interface was much lower than that at the soybean oil/water interface, and the overall trend of interfacial tension decreases with the increase of the content of litsea cubeba oil. Lower interfacial tension indicates more balanced hydrophobic surfaces of proteins, resulting in smaller droplets and higher emulsion stability (Alavia et al., 2021; Carranza et al., 2016). These results reflected that the protein owned stronger adsorption capacity and accumulated more at the flavor oil/water interface. This result might be related to the content of aromatic compounds in the oil phase. Bi et al. (S. Bi et al., 2022) reported that (Z) −2-pentene-1-ol, hexal, and (E) −2-octylal could spontaneously interact with pea proteins. Guo et al. (Guo et al., 2020) found that high concentrations of citronellal, citronellin acetate, citronellyl propionate and citronellin could induce conformational changes in protein when binding. Citral has been reported to form

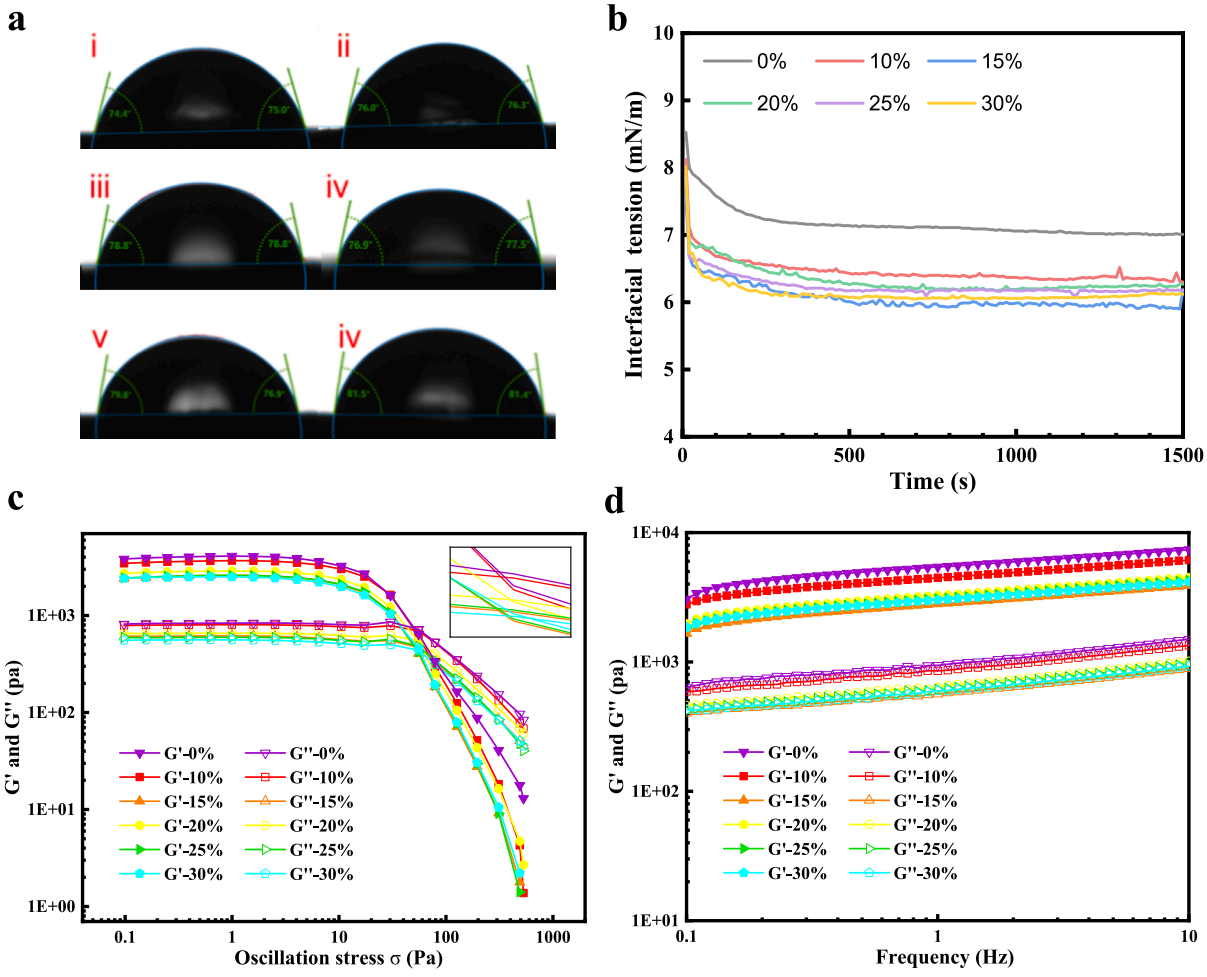

Fig. 2. a: Three-phase contact angle of GOS-GCP (*i ~ vi: Oil phase contained 0%, 10%, 15%, 20%, 25% and 30% litsea cubeba oil); b: The interfacial tension of GOS-GCP at different ratios litsea cubeba oil/water interface; c: Stress curve of HIPEs; d: Frequency curve of HIPEs.

covalent compounds with β-lactoglobulin (Anantharamkrishnan & Reineccius, 2020). Therefore, it can be inferred that the flavor compounds in litsea cubeba oil could combine with the hydrophobic groups of the interfacial proteins to form a more stable interfacial layer and reduce the damage caused by the ice crystals to the emulsion droplets during the freezing process.

The interaction between droplets can affect the stability of emulsion during freeze–thaw process. The rheological behavior of flavor HIPEs were measured by rheometer, and the linear viscoelastic region and yield behavior of emulsions were analyzed by oscillation stress sweeps. As shown in Fig. 2c, the storage modulus (G′) of flavor HIPEs was dominant over the loss modulus (G″), exhibiting a clear gel-like behavior (Hu et al., 2021). In addition, G′ and G″ in the linear viscoelastic region were both independent of the increase of stress amplitude, and the same phenomenon can also be observed in HIPEs independent frequency sweep curves with the increase of frequency (Fig. 2d), reflecting that flavor HIPEs has a strong gel-like behavior due to strong interaction between droplets (Moakes et al., 2015).

The G′ and G″ of all samples decreased with the continuous increase of the oscillatory stress, during which they intersected at a point, and the stress corresponding to the intersection point was defined as the yield stress, indicating the broke down of the gel-like network structure. When the stress increased further, G″ > G′, illustrated the structure rearrangement of emulsion droplets, and the rheological behavior of HIPEs changed from elastic to viscosity (Burchard, 1999). Furthermore, with the increase of litsea cubeba oil content, there was little difference in yield stress, indicating that flavor HIPEs had similar ability to resist stress, and there was no significant difference in the interaction between emulsion droplets.

In the linear viscoelastic region, a decrease in the viscoelastic was observed with the addition of litsea cubeba oil (Fig. 2c&d), illustrated that the addition of high concentration of litsea cubeba oil enhanced the flexibility of the emulsion gel-like network structure, hence the emulsion could better cope with the damage of ice crystals to the interfacial layer

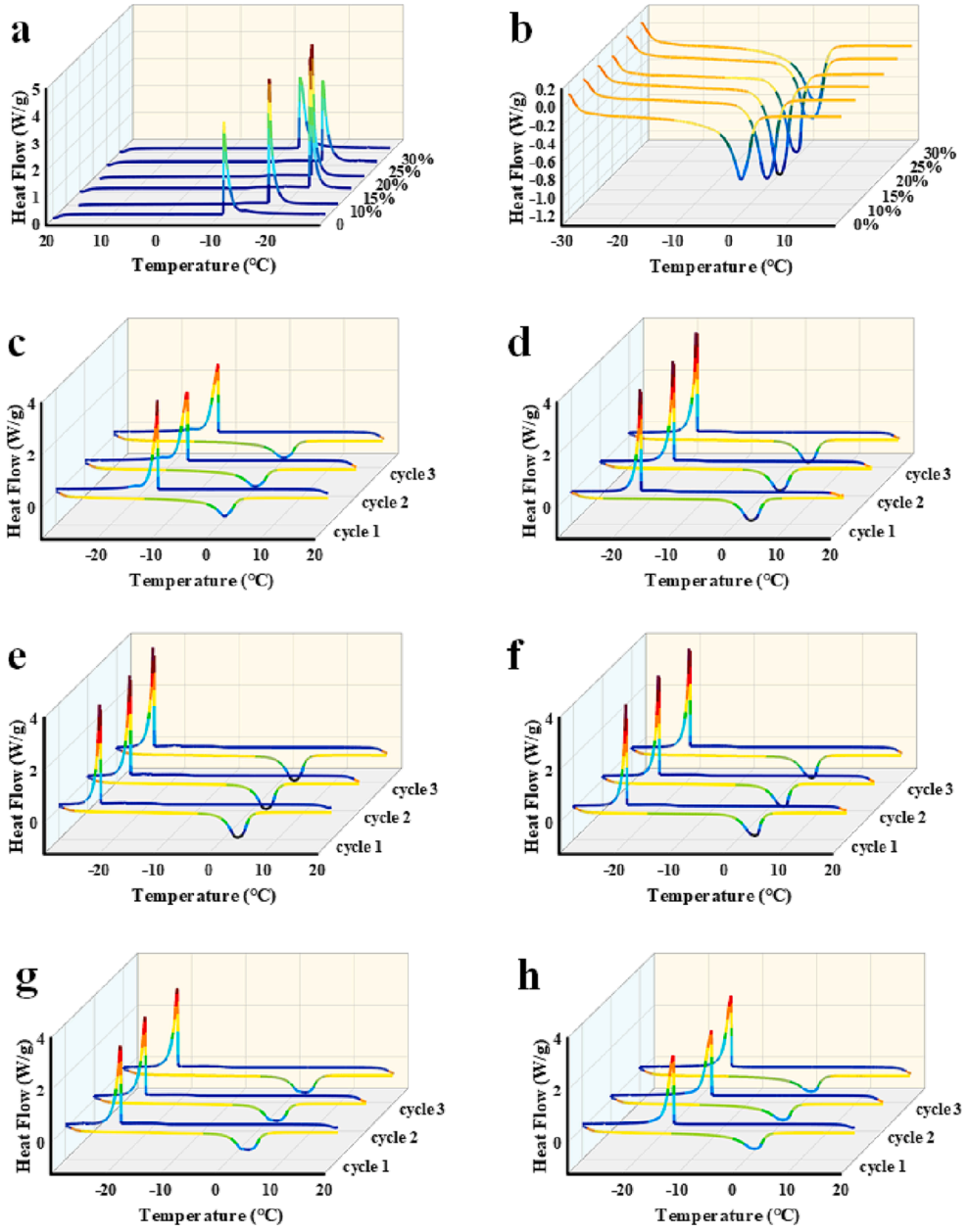

Fig. 3. a & b DSC curve of cooling (a) and heating (b) process of HIPEs with different content of litsea cubeba oil in oil phase; c ~ h: 3 freeze–thaw cycles of HIPEs with 0% (c), 10%(d), 15%(e), 20%(f), 25% (g), 30% (h) litsea cubeba oil in oil phase.

during the freezing process.

In this study, the crystallization behavior and phase transition of HIPEs during freeze–thaw process were analyzed by DSC, in order to further explore the freeze–thaw stability of flavor HIPEs. The heating and cooling curves of HIPEs are shown in Fig. 3a&b. The exothermic peaks of the samples were relatively dispersed, and the temperature of the peaks varied from −10 °C to –22 °C, while the temperature of the endothermic peaks ranged from 0 °C to 2 °C which was caused by the phase transition as a result of ice crystals melting in the aqueous phase of HIPEs, in agreement with other works (Palazolo et al., 2011). Therefore, the exothermic peak in the cooling curve in Fig. 3a was considered as the phase transition caused by the formation of ice crystals of aqueous phase. Therefore, the instability of HIPEs after freeze–thaw process was mainly due to the crystallization of aqueous phase during the freezing process. The formation of ice crystals destroyed the oil/water interfacial layer, which leaded to the coalescence between droplets (Palazolo et al., 2011). In addition, due to the freezing of the aqueous phase, the unfrozen solute was concentrated, and the high concentration of protein could be separated from the aqueous phase due to the decrease of unfrozen water and be confined to the crystals, thus leading to the decrease of stabilizer between the emulsion droplets and the occurrence of droplet aggregation (Schroeder et al., 2017). In addition, the oil phase had a significant effect on the enthalpy change (ΔHT) of the endothermic and exothermic peak of HIPEs (Fig. 3a&b). With the increase of the litsea cubeba oil content, ΔHT in the heating and cooling process of HIPEs decreased significantly, indicating that the amount of ice crystals formed was reduced (Huang et al., 2022). This conclusion could be explained by the decrease of aqueous crystallization point after protein binding with flavor substance. Moreover, the temperature of the endothermic peak of the HIPEs added with litsea cubeba oil was far away from 0 °C, reflecting that flavor HIPEs were less damaged by ice crystals, which was consistent with the previously observed freeze–thaw stability of HIPEs (Fig. 1). Fig. 3c ~ h exhibits the endothermic and exothermic curves of the HIPEs after 3 freeze–thaw cycles. The ΔHT changed of the HIPEs containing more than 15% litsea cubeba oil were not obvious, indicating that the degree of emulsion phase transition was almost constant, and the emulsion structure was relatively stable.

To sum up, the better freezing-thawing stability of HIPEs with high content of litsea cubeba oil could be interpreted as the increased hydrophobicity of protein binding with flavor substances and the decreased surface tension, which promoted the rapid adsorption of more proteins to the oil/water interface to form a more stable interface layer. After binding with flavor substance, the protein reduced the aqueous crystallization point of emulsion and reduced the formation of ice crystals during freezing. The emulsion gel-like network structure was more flexible, which could resist the damage of the formed ice crystal to the interface layer.

3.3. Preservation of flavor substances by HIPEs after freeze–thaw process

In order to determine the retention and release of flavor substances embedded in HIPEs after freeze–thaw process, SPME was used to extracted the flavor substances of HIPEs containing 30% litsea cubeba oil in the oil phase, and GC–MS was used to analyzed the qualitative and quantitative of volatile flavor compounds in HIPEs. By comparing the non-polar RI value, molecular weight, and the matching degree between flavor substances and the National Institute of Science and Technology (NIST) standard reference data, 26 volatile compounds in flavor HIPEs were determined, and the qualitative information is exhibited in Table S1. As shown in the pie chart (Fig. 4a), the flavor of HIPEs were mainly composed of 2,6-Octadien-1-ol, 3,7-dimethyl-, (Z/E)- (81.10%), D-limonene (8.58%), β-Myrcene (1.66%), β-pinene (1.38%), α-pinene (1.27%), α-Cyclocitral (1.10%) and 5-Hepten-2-one, 6-methyl- (0.89%), and the remaining 19 substances accounted for 4.02% in total, in agreement with other works (Li et al., 2014).

The results of the quantitative detection of 26 flavor substances of HIPEs after 5 freeze–thaw cycles were summarized in Table 1. A heat map visually shows the relationship between the release of flavor substances in HIPEs after several freeze–thaw cycles (Fig. 4b), and the results revealed that there was little difference in the flavor release of HIPEs after one freeze–thaw cycle and that of HIPEs after 5 freeze–thaw cycles. The high amount of low molecular weight flavor substances detected after three freeze–thaw cycles might be caused by the difference in the emulsion preparation process. Moreover, the release of four flavor substances with higher content, i.e., 2,6-Octadien-1-ol, 3,7-dimethyl-, (Z)-, 2,6-Octadien-1-ol, 3,7-dimethyl-, (E)-, D-limonene and β-Myrcene, before and after freezing-thawing was compared (Fig. 4c ~ f), and the results reflected that encapsulation can effectively slow down the release of flavor substances, and the freeze–thaw stable HIPEs prepared in this study play a key role in the preservation of flavor substances during the freeze–thaw process.

3.4. Application of freeze–thaw stabilized flavor HIPEs in 3D printing

As a 3D printing ink, the HIPEs need to have good extrudability, and can cure quickly when setting after extrusion. However, materials usually undergo major degeneration in the process of 3D printing, hence the deformation and response ability of HIPEs were researched. As shown in Fig. 5a, in each of the three periods, G′ of flavor HIPEs remained almost unchanged with time, and the thixotropic recovery rates of HIPEs were 81.6%, 71.3%, 79.4%, 73.0%, 73.9% and 75.6% (the content of litsea cubeba oil in oil phase was 0% and 10%~30%, respectively), which were all over 70%, indicated that flavor HIPEs had good thixotropic recovery (Patel & Dewettinck, 2015; J. Wu et al., 2022), and could be applied to 3D printing.

HIPEs constructed with GOS-GCP and different proportions of litsea cubeba oil showed perfect self-supporting and were able to prepare high-resolution 3D printed objects (Fig. 5b), which might be due to the development of intermolecular covalent crosslinking networks (Li et al., 2020). It can be observed that the HIPEs 3D printed object with 10% litsea cubeba oil has a small amount of oil separated out at the bottom after 3 freeze–thaw cycles, but the overall structure remains intact; however, after 5 freeze–thaw cycles, the bottom of the 3D printed object was not strong enough to support the superstructure. At the same time, slight oil precipitation, which could be seen by the oil reflection, occurred at the bottom of HIPEs without adding litsea cubeba oil. In contrast, the 3D printed objects prepared by HIPEs with 15% or more litsea cubeba oil still maintained high resolution and integrity after 5 freeze-thaws, indicating that flavor HIPEs can be used as a freeze–thaw stable ink in the development of 3D printed products. The above results might be due to the different properties of protein at the flavor oil/water interface and lateral attractive capillary forces of protein particles at the interface (Berton-Carabin & Schroen, 2015).

4. Conclusions

In this study, the flavor HIPEs system was constructed by adding different proportions of litsea cubeba oil into the oil phase. The results showed that HIPEs containing litsea cubeba oil were endowed with the greatest potential for preparing food-grade 3D printing objects with high freeze–thaw stability. The binding of proteins and flavor substances at the oil–water interface improved the stability of HIPEs, and the protein denaturation leads to the reduction of the formation of ice crystals; HIPEs and gel network structures are more flexible and can resist the damage of ice crystals to droplets. The specific mechanism of protein binding to flavor substance needs further study. Moreover, it was also found that the constructed HIPEs system had the ability of preserving flavor substances during freeze–thaw process. Overall, this study provides a new method for the preservation of flavor substances under freezing conditions and expands the application range of flavor HIPEs in food industry.

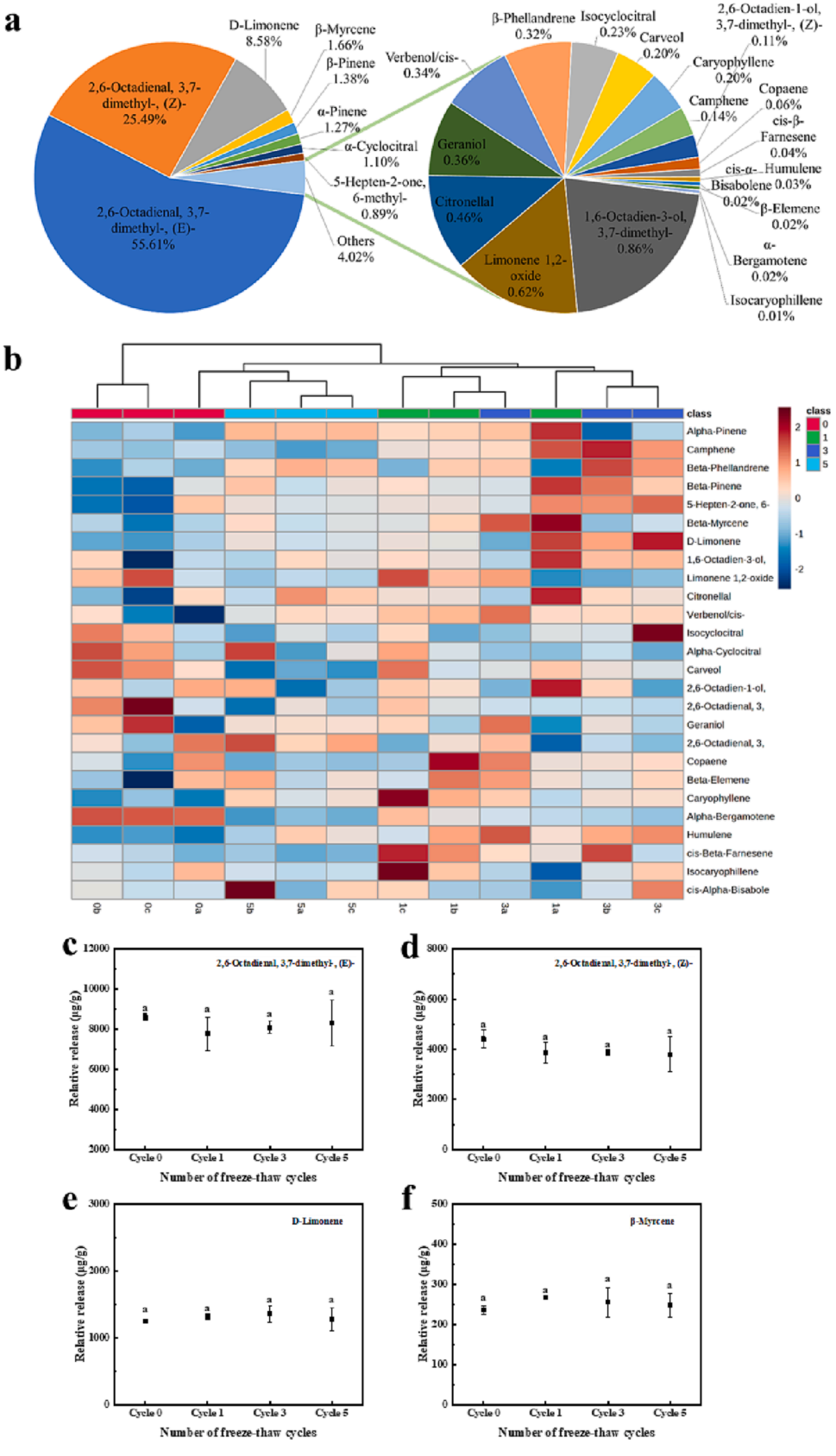

Fig. 4. a: Proportion of flavor compounds in flavor HIPEs; b: Two-dimensional hierarchical cluster analysis of flavor compounds of HIPEs (*The most and least intense relative abundance values are depicted in red and blue, respectively); c ~ f: Changes of flavor release of four main flavor compounds after freeze–thaw cycles (*Different letters indicated significant differences between different samples, $p < 0.05$). (For interpretation of the references to colour in this figure legend, the reader is referred to the web version of this article.)

Table 1
HIPEs flavor relative release before and after freeze–thaw cycles.

No.	Compound	Relative release (μg/g)			
		Cycle 0	Cycle 1	Cycle 3	Cycle 5
1	α-Pinene	153.93 ± 12.01 a	187.92 ± 0.38 a	154.74 ± 31.71 a	189.20 ± 27.19 a
2	Camphene	23.47 ± 0.51 bc	25.99 ± 0.01 ab	28.74 ± 1.73 a	20.52 ± 2.44 c
3	β-Phellandrene	38.42 ± 3.78 a	38.17 ± 8.80 a	51.67 ± 2.08 a	48.42 ± 8.46 a
4	β-Pinene	156.72 ± 36.17 b	224.77 ± 14.70 a	228.27 ± 21.20 a	206.06 ± 13.54 ab
5	5-Hepten-2-one, 6-methyl-	109.51 ± 33.55 b	142.50 ± 0.86 ab	157.78 ± 17.71 a	132.37 ± 17.32 ab
6	β-Myrcene	236.04 ± 10.48 a	267.53 ± 4.92 a	255.55 ± 37.26 a	248.41 ± 29.69 a
7	D-Limonene	1255.38 ± 29.54 a	1322.80 ± 44.40 a	1361.28 ± 125.03 a	1280.81 ± 174.26 a
8	1,6-Octadien-3-ol, 3,7-dimethyl-	125.51 ± 11.18 a	132.77 ± 4.80 a	131.67 ± 4.06 a	128.86 ± 22.83 a
9	Limonene 1,2-oxide	105.46 ± 8.28 a	95.69 ± 16.30 a	93.33 ± 8.44 a	91.96 ± 14.55 a
10	Citronellal	60.39 ± 7.18 a	67.91 ± 0.55 a	64.31 ± 1.54 a	68.72 ± 14.76 a
11	Verbenol/cis-	43.77 ± 7.63 a	52.42 ± 5.99 a	54.56 ± 4.51 a	51.00 ± 8.78 a
12	Isocyclocitral	38.39 ± 2.30 a	33.49 ± 3.29 a	36.33 ± 3.78 a	33.66 ± 6.09 a
13	α-Cyclocitral	183.16 ± 15.54 a	160.79 ± 23.36 a	154.03 ± 3.44 a	163.88 ± 8.29 a
14	Carveol	43.82 ± 3.42 a	38.49 ± 5.06 a	36.28 ± 0.77 a	30.08 ± 5.69 a
15	2,6-Octadien-1-ol, 3,7-dimethyl-, (Z)-	21.14 ± 1.73 a	21.43 ± 0.90 a	16.58 ± 2.16b	16.34 ± 1.44 b
16	2,6-Octadienal, 3,7-dimethyl-, (Z)-	4416.75 ± 358.84 a	3861.08 ± 417.37 a	3866.84 ± 110.87 a	3804.60 ± 704.64 a
17	Geraniol	58.29 ± 31.08 a	41.29 ± 15.99 a	56.71 ± 15.58 a	54.22 ± 8.35 a
18	2,6-Octadienal, 3,7-dimethyl-, (E)-	8622.13 ± 148.22 a	7784.51 ± 834.61 a	8086.22 ± 303.63 a	8300.44 ± 1144.40 a
19	Copaene	9.40 ± 0.36 a	9.07 ± 1.16 a	9.27 ± 0.51 a	8.55 ± 1.36 a
20	β-Elemene	2.57 ± 0.36 a	2.75 ± 0.36 a	2.82 ± 0.22 a	2.73 ± 0.25 a
21	Caryophyllene	26.31 ± 2.17 a	32.58 ± 6.81 a	30.57 ± 1.46 a	29.91 ± 3.50 a
22	α-Bergamotene	4.13 ± 0.13 a	3.06 ± 0.49 b	2.79 ± 0.17 b	2.51 ± 0.46 b
23	Humulene	3.19 ± 0.18 b	3.79 ± 0.46 ab	4.34 ± 0.27 a	3.76 ± 0.78 ab
24	*cis*-β-Farnesene	6.10 ± 0.49 ab	7.71 ± 1.60 a	7.10 ± 0.91 ab	5.31 ± 0.57 b
25	Isocaryophillene	0.90 ± 0.05 a	0.89 ± 0.30 a	0.84 ± 0.05 a	0.80 ± 0.11 a
26	*cis*-α-Bisabolene	2.46 ± 0.08 a	2.11 ± 0.69 a	2.61 ± 0.64 a	2.89 ± 0.67 a

*Different letters indicated significant differences between different samples, $p < 0.05$.

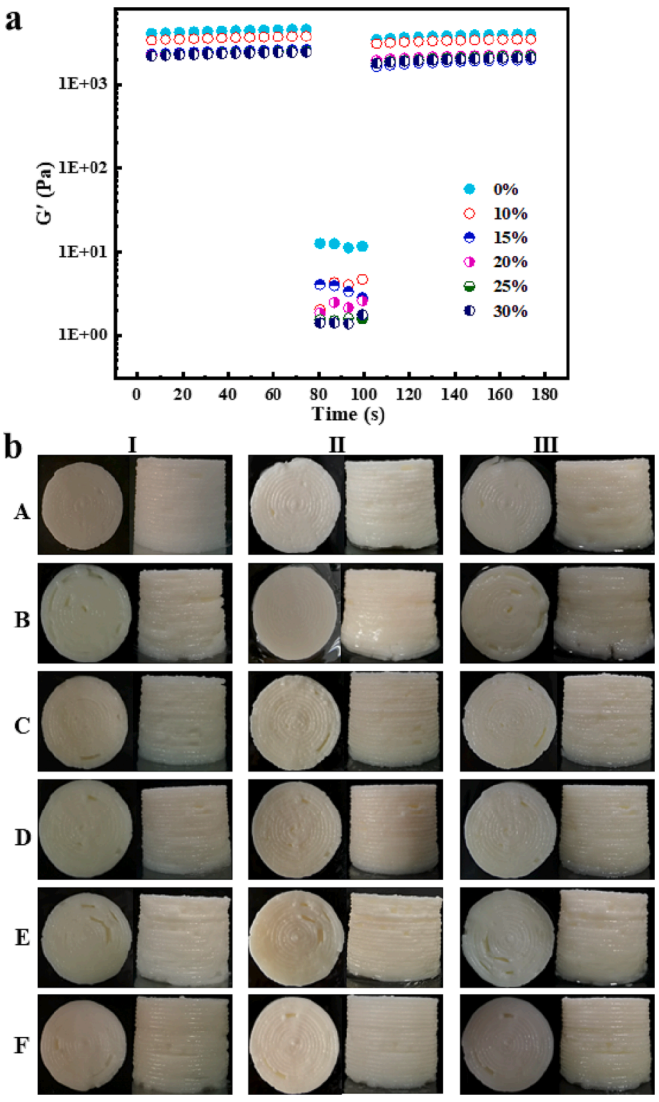

Fig. 5. a: The thixotropic recovery of falvor HIPEs; b: Visual observation of 5 freeze–thaw cycles of the 3D objects printed by HIPEs (*A ~ F: 3D printed objects using HIPEs with 0%, 10%, 15%, 20%, 25% and 30% litsea cubeba oil in the oil phase oil, respectively; I ~ III: 3D printed objects after 0, 3 and 5 freeze–thaw cycles).

CRediT authorship contribution statement

Sijie Hu: Investigation, Data curation, Writing – original draft, Writing – review & editing. **Feng Xiao:** Investigation, Formal analysis. **Ming Du:** Supervision, Visualization. **Jinfeng Pan:** Validation, Visualization. **Liang Song:** Resources, Investigation. **Chao Wu:** Software, Project administration. **Beiwei Zhu:** Conceptualization, Resources. **Xianbing Xu:** Conceptualization, Methodology, Funding acquisition.

Declaration of Competing Interest

The authors declare the following financial interests/personal relationships which may be considered as potential competing interests: Xian-Bing Xu reports financial support was provided by National Natural Science Foundation of China (Grant No. 32072261).

Data availability

Data will be made available on request.

Acknowledgments

This work was supported by the National Natural Science Foundation of China (Grant No. 32072261).

Appendix A. Supplementary data

Supplementary data to this article can be found online at https://doi.org/10.1016/j.fochx.2023.100759.

References

Alavia, W., Lovera, J. A., Graber, T. A., Azúa, D., & Soto, I. (2021). Modeling of the density, viscosity and electrical conductivity of aqueous solutions saturated in boric acid in presence of lithium sulfate or sodium sulfate at 293.15 to 313.15 K. *Fluid Phase Equilibria, 532*, Article 112864. https://doi.org/10.1016/j.fluid.2020.112864

Ali, M. H., Issayev, G., Shehab, E., & Sarfraz, S. (2022). A critical review of 3D printing and digital manufacturing in construction engineering. *Rapid Prototyping Journal, 28*(7), 1312–1324. https://doi.org/10.1108/rpj-07-2021-0160

Anantharamkrishnan, V., & Reineccius, G. A. (2020). Influence of pH, temperature, and water activity on covalent adduct formation between selected flavor compounds and model protein β-lactoglobulin. *Journal of Agricultural and Food Chemistry, 68*(47), 13833–13843. https://doi.org/10.1021/acs.jafc.0c06752

Atkins, C. J., Seow, D. K., Burns, G., Town, J. S., Hand, R. A., Lester, D. W., … Eissa, A. M. (2020). Branched macromonomers from catalytic chain transfer polymerisation (CCTP) as precursors for emulsion-templated porous polymers. *Polymer Chemistry, 11*. https://doi.org/10.1039/D0PY00539H

Berton-Carabin, C. C., & Schroen, K. (2015). Pickering emulsions for food applications: Background, trends, and challenges. *Annual Review of Food Science and Technology, 6*, 263–297. https://doi.org/10.1146/annurev-food-081114-110822

Bi, A., Xu, X., Guo, Y., Du, M., Yu, C., & Wu, C. (2022). Fabrication of flavour oil high internal phase emulsions by casein/pectin hybrid particles: 3D printing performance. *Food Chemistry, 371*(Mar. 1), Article 131349. https://doi.org/10.1016/j.foodchem.2021.131349

Bi, S., Pan, X., Zhang, W., Ma, Z., Lao, F., Shen, Q., & Wu, J. (2022). Non-covalent interactions of selected flavors with pea protein: Role of molecular structure of flavor compounds. *Food Chemistry, 389*(Sep. 30), 389. https://doi.org/10.1016/j.foodchem.2022.133044

Burchard, W. (1999). Solution properties of branched macromolecules. *Advances in Polymer Science, 143*, 114–194. https://doi.org/10.1007/3-540-49780-3_3

Carranza, A., Song, K., Soltero-Martínez, J. F. A., Wu, Q., Pojman, J. A., & Mota-Morales, J. D. (2016). On the stability and chemorheology of a urea choline chloride deep-eutectic solvent as an internal phase in acrylic high internal phase emulsions. *RSC Advances, 6*(85), 81694–81702. https://doi.org/10.1039/c6ra18931h

Dong, X., Huang, Y., Pan, Y., Wang, K., Prakash, S., & Zhu, B. (2019). Investigation of sweet potato starch as a structural enhancer for three-dimensional printing of Scomberomorus niphonius surimi. *Journal of Texture Studies, 50*(4), 316–324. https://doi.org/10.1111/jtxs.12398

Du, J., Dai, H., Wang, H., Yu, Y., Zhu, H., Fu, Y., … Zhang, Y. (2021). Preparation of high thermal stability gelatin emulsion and its application in 3D printing. *Food Hydrocolloids, 113*, Article 106536. https://doi.org/10.1016/j.foodhyd.2020.106536

Enfield, R. E., Pandya, J. K., Lu, J., McClements, D. J., & Kinchla, A. J. (2022). The future of 3D food printing: Opportunities for space applications. *Critical Reviews in Food Science and Nutrition, 1–14*. https://doi.org/10.1080/10408398.2022.2077299

Ghosh, S., & Coupland, J. N. (2008). Factors affecting the freeze–thaw stability of emulsions. *Food Hydrocolloids*, *22*(1), 105-111. doi: Factors affecting the freeze–thaw stability of emulsions.

Guo, J., He, Z., Wu, S., Zeng, M., & Chen, J. (2020). Effects of concentration of flavor compounds on interaction between soy protein isolate and flavor compounds. *Food Hydrocolloids, 100*, Article 105388. https://doi.org/10.1016/j.foodhyd.2019.105388

Hu, S., Wu, J., Zhu, B., Du, M., Wu, C., Yu, C., … Xu, X. (2021). Low oil emulsion gel stabilized by defatted Antarctic krill (Euphausia superba) protein using high-intensity ultrasound. *Ultrasonics Sonochemistry, 70*, Article 105294. https://doi.org/10.1016/j.ultsonch.2020.105294

Huang, Z. X., Lin, W., Zhang, Y., & Tang, C.-H. (2022). Outstanding freeze-thaw stability of mayonnaise stabilized solely by a heated soy protein isolate. *Food Biophysics, 17*(3), 335–343. https://doi.org/10.1007/s11483-022-09722-1

Li, W. R., Shi, Q. S., Liang, Q., Xie, X. B., Huang, X. M., & Chen, Y. B. (2014). Antibacterial activity and kinetics of Litsea cubeba oil on Escherichia coli. *PLoS One, 9*, 5–10. https://doi.org/10.1371/journal.pone.0110983

Li, X., Xu, X., Song, L., Bi, A., Wu, C., Ma, Y., … Zhu, B. (2020). High internal phase emulsion for food-grade 3D printing materials. *Acs Applied Materials & Interfaces, 12*(40), 45493–45503. https://doi.org/10.1021/acsami.0c11434

Lissant, K. J. (1966). The geometry of high-internal-phase-ratio emulsions. *Journal of Colloid and Interface Science, 22*, 462–468. https://doi.org/10.1016/0021-9797(66)90091-9

Liu, X., Guo, J., Wan, Z. L., Liu, Y. Y., Ruan, Q. J., & Yang, X. Q. (2018). Wheat gluten-stabilized high internal phase emulsions as mayonnaise replacers. *Food Hydrocolloids, 77*, 168–175. https://doi.org/10.1016/j.foodhyd.2017.09.032

Manfredini, N., Merigo, M., Ilare, J., Sponchioni, M., & Moscatelli, D. (2021). Limonene-in-water Pickering emulsion and on-demand separation using thermo-responsive biodegradable nanoparticles. *Nanoscale, 13*(18), 8543–8554. https://doi.org/10.1039/d1nr00694k

Mao, L., Roos, Y. H., Biliaderis, C. G., & Miao, S. (2017). Food emulsions as delivery systems for flavor compounds: A review. *Critical Reviews in Food Science and Nutrition, 57*(15), 3173–3187. https://doi.org/10.1080/10408398.2015.1098586

Marcuzzo, E., Debeaufort, F., Sensidoni, A., Tat, L., Beney, L., Hambleton, A., … Voilley, A. (2012). Release behavior and stability of encapsulated D-limonene from emulsion-based edible films. *Journal of Agricultural and Food Chemistry, 60*(49), 12177–12185. https://doi.org/10.1021/jf303327n

Moakes, R. J. A., Sullo, A., & Norton, I. T. (2015). Preparation and rheological properties of whey protein emulsion fluid gels. *Rsc Advances, 5*(75), 60786–60795. https://doi.org/10.1039/c5ra12684c

Noshad, M., Mohebbi, M., Shahidi, F., & Koocheki, A. (2015). Freeze–thaw stability of emulsions with soy protein isolate through interfacial engineering. *International Journal of Refrigeration, 58*, 253–260. https://doi.org/10.1016/j.ijrefrig.2015.05.007

Oliver, C. M., Kher, A., McNaughton, D., & Augustin, M. A. (2009). Use of FTIR and mass spectrometry for characterization of glycated caseins. *Journal of Dairy Research, 76*, 105–110. https://doi.org/10.1017/S002202990800383X

Palazolo, G. G., Sobral, P. A., & Wagner, J. R. (2011). Freeze-thaw stability of oil-in-water emulsions prepared with native and thermally-denatured soybean isolates. *Food Hydrocolloids, 25*(3), 398–409. https://doi.org/10.1016/j.foodhyd.2010.07.008

Patel, A. R., & Dewettinck, K. (2015). Comparative evaluation of structured oil systems: Shellac oleogel, HPMC oleogel, and HIPE gel. *European Journal of Lipid Science and Technology, 117*(11), 1772–1781. https://doi.org/10.1002/ejlt.201400553

Petrovic, V., Vicente Haro Gonzalez, J., Jordá Ferrando, O., Delgado Gordillo, J., Ramón Blasco Puchades, J., & Portolés Griñan, L. (2010). Additive layered manufacturing: sectors of industrial application shown through case studies. *International Journal of Production Research*, *49*(4), 1061-1079. doi: 10.1080/00207540903479786.

Purwanti, N., Ichikawa, S., Neves, M. A., Uemura, K., Nakajima, M., & Kobayashi, I. (2016). B-Lactoglobulin as food grade surfactant for clove oil-in-water and limonene-in-water emulsion droplets produced by microchannel emulsification. *Food Hydrocolloids, 60*, 98–108. https://doi.org/10.1016/j.foodhyd.2016.03.024

Saifullah, M., Shishir, M. R. I., Ferdowsi, R., Tanver Rahman, M. R., & Van Vuong, Q. (2019). Micro and nano encapsulation, retention and controlled release of flavor and aroma compounds: A critical review. *Trends in Food Science and Technology, 86*, 230–251. https://doi.org/10.1016/j.tifs.2019.02.030

Schroeder, W. F., Williams, R. J. J., Hoppe, C. E., & Romeo, H. E. (2017). Unidirectional freezing as a tool for tailoring air permeability in macroporous poly(ethylene glycol)-based cross-linked networks. *Journal of Materials Science, 52*(23), 13669–13680. https://doi.org/10.1007/s10853-017-1460-4

Sears, N. A., Dhavalikar, P. S., & Cosgriff-Hernandez, E. M. (2016). Emulsion inks for 3D printing of high porosity materials. *Macromolecular Rapid Communications, 37*(16), 1369–1374. https://doi.org/10.1002/marc.201600236

Wan, Y., Wang, R., Feng, W., Chen, Z., & Wang, T. (2021). High internal phase Pickering emulsions stabilized by co-assembled rice proteins and carboxymethyl cellulose for food-grade 3D printing. *Carbohydrate Polymers, 273*, Article 118586. https://doi.org/10.1016/j.carbpol.2021.118586

Wang, H., Ouyang, Z., Hu, L., Cheng, Y., Zhu, J., Ma, L., & Zhang, Y. (2022). Self-assembly of gelatin and phycocyanin for stabilizing thixotropic emulsions and its effect on 3D printing. *Food Chemistry, 397*, Article 133725. https://doi.org/10.1016/j.foodchem.2022.133725

Wang, Y., Zhang, A., Wang, X., Xu, N., & Jiang, L. (2020). The radiation assisted-Maillard reaction comprehensively improves the freeze-thaw stability of soy protein-stabilized oil-in-water emulsions. *Food Hydrocolloids, 103*, Article 105684. https://doi.org/10.1016/j.foodhyd.2020.105684

Wu, J., Guan, X., Wang, C., Ngai, T., & Lin, W. (2022). pH-Responsive Pickering high internal phase emulsions stabilized by Waterborne polyurethane. *Journal of Colloid and Interface Science, 610*, 994–1004. https://doi.org/10.1016/j.jcis.2021.11.156

Wu, K., Shi, Z., Liu, C., Su, C., Zhang, S. X., & Yi, F. (2022). Preparation of Pickering emulsions based on soy protein isolate-tannic acid for protecting aroma compounds and their application in beverages. *Food Chemistry, 390*, Article 133182. https://doi.org/10.1016/j.foodchem.2022.133182

Wu, X., Liu, X., Qin, J., Zhou, J., & Chen, J. (2022). Controlled flavor release from high internal phase emulsions as fat mimetics based on glycyrrhizic acid and phytosterol. *Food Research International, 161*, Article 111810. https://doi.org/10.1016/j.foodres.2022.111810

Zhang, B., Zhang, J., Yu, X., Peng, J., Pan, L., & Tu, K. (2022). Evaluation of the adsorption capacity and mechanism of soy protein isolate for volatile flavor compounds: Role of different oxygen-containing functional groups. *Food Chemistry, 386*. https://doi.org/10.1016/j.foodchem.2022.132745